Carbohydrate Polymers 87 (2012) 300–308

Contents lists available at ScienceDirect

Carbohydrate Polymers

journal homepage: www.elsevier.com/locate/carbpol

Magnetically controlled release of cisplatin from superparamagnetic starch nanoparticles

Sweta Likhitkar, A.K. Bajpai*

Bose Memorial Research Laboratory, Department of Chemistry, Government Autonomous Science College, Jabalpur, MP 482003, India

ARTICLE INFO

Article history:
Received 27 February 2011
Received in revised form 27 June 2011
Accepted 26 July 2011
Available online 3 August 2011

Keywords:
Cisplatin
Starch
Iron oxide
Nanoparticles
Super-paramagnetic
Drug delivery
Anticancer

ABSTRACT

The present study involves a novel strategy for the preparation of superparamagnetic nanoparticles of crosslinked starch impregnated with homogeneously dispersed nanosized iron oxide. The nanoparticles were loaded with an anticancer drug 'cisplatin' and the drug release kinetics was investigated spectrophotometrically at physiological pH (7.4). The nanoparticles were characterized by Fourier transform infra red (FTIR) spectroscopy, transmission electron microscopy (TEM), X-ray diffraction and magnetization studies. The particle size of magnetic starch nanoparticles was found to lie in the range of 20–90 nm. The influence of factors like chemical composition of nanoparticles, pH and temperature of the release media and applied magnetic field was investigated on the release profiles of the drug. The prepared nanoparticles could provide a possible pathway for targeted and controlled delivery of anticancer drugs minimizing side effects and achieving higher efficacy.

1. Introduction

Recent past has witnessed an increasing use of magnetic nanoparticles such as magnetite (Fe_3O_4), maghemite (γFe_2O_3), ferrites etc., for various biomedical applications. Iron oxide nanoparticles have very high magnetization as close to that of bulk Fe (218 emu/g) (Taylor et al., 2010) and, therefore, have been suggested for these applications (Babincova, Leszczynska, Sourivong, Cicmanec, & Babinec, 2001; Jordan, Scholz, Wust, Hling, & Felix, 1999) like controlled drug release (Müller-Schulte & Schmitz-Rode, 2006; Wang et al., 2006), contrast, enhancement agents in magnetic resonance imaging (Couvreur, Barratt, Fattal, Legrand, & Vauthier, 2002; Hu et al., 2006).

Biocompatible and biodegradable drug delivery systems can preferably be made of naturally occurring polymers such as chitosan, gelatin, polysaccharides and silk fibroin (Bertholon, Hommel, Labarre, & Vauthier, 2006; Ethirajan, Schoeller, Musyanovych, Ziener, & Landfester, 2008; Prato, Kostarelos, & Bianco, 2008; Wang, 2009; Wenk, Wandrey, Merkle, & Meinel, 2008; Zhang, Mardyani, Chan, & Kumacheva, 2006). The major limitation of current anticancer drugs is their toxicity and lack of specificity. In an attempt to overcome these problems endocytosable carriers such as microsphere, liposomes and nanoparticles have been suggested to make the treatment more effective (Sangeetha, Harish, & Samanta, 2010). Chemotherapy with cisplatin is associated with various secondary effects, such as anemia, nausea, vomiting, neurotoxicity and nephrotoxicity (Uchino et al., 2005). Due to these side effects alternative methods of administering cisplatin are needed. In the present study, starch has been selected as the raw material to prepare the drug carrier because of its biocompatibility, biodegradability, and inert nature.

Cisplatin is an inorganic compound containing a platinum atom surrounded in plane by 2 anions of chloride and 2 amino groups in *cis* position. Cisplatin remains a front line drug for the treatment of solid epithelial tumors, but causes nephrotoxicity.

In the present study, we have synthesized and characterized cisplatin containing iron-oxide impregnated starch nanoparticles as a possible and potential drug carrier for magnetically mediated targeted drug delivery. The proposed objectives of the present work have been schematically depicted in Fig. 1(A) and (B). Whereas the image (A) describes the binding of cisplatin molecules to the iron oxide impregnated starch nanoparticles, the image (B) visualizes its possible applications in targeting infected cells by applying external magnetic field to enable the release of the drug from the drug-loaded nanoparticles.

If a magnetic material is placed in a magnetic field of strength H, the individual atomic moments in the material contribute to its overall response. The magnetic induction is given by the following relation

$$B = \mu_0(H + M) \quad (1)$$

* Corresponding author.
E-mail addresses: akbmrl@yahoo.co.in, akbajpailab@yahoo.co.in (A.K. Bajpai).

0144-8617/$ – see front matter © 2011 Elsevier Ltd. All rights reserved.
doi:10.1016/j.carbpol.2011.07.053

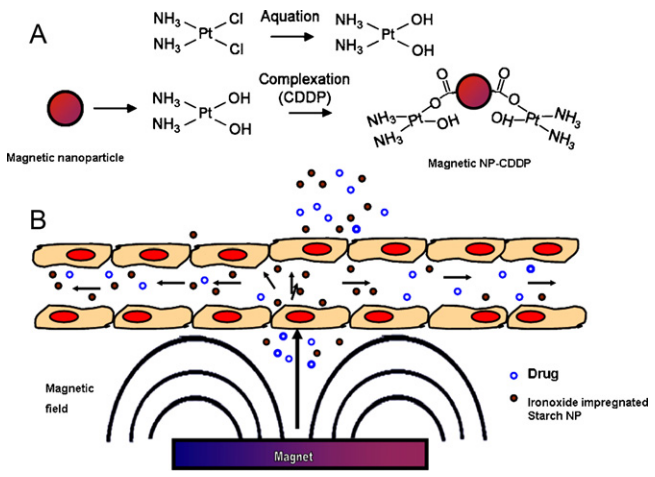

Fig. 1. Schematic presentation of (A) binding of cisplatin drug molecules to the iron oxide impregnated starch nanoparticles, and (B) possible targeting of cells by released drug due to applied magnetic field.

where μ_o is the permeability of free space, and the magnetization $M = m/v$ is the magnetic moment per unit volume, m is the magnetic moment for volume v of the material. All materials are magnetic to some extent with their response depending on their atomic structure and temperature. They may be conveniently classified in terms of their volumetric magnetic susceptibility, χ where

$$M = \chi_m H \quad (2)$$

describes the magnetization induced in a material by H. In SI unit χ_m is dimension less and both M and H are expressed in Am^{-1}. Most materials display little magnetism, and even then only in the presence of applied field. The susceptibility in ordered materials depends not just on temperature but also on H, which gives rise to the sigmoidal shape of the M–H curve, with M approaching a saturation value at large value of H (Morrish, 2001).

2. Experimental

2.1. Materials

Water-soluble starch was purchased from E. Merck, Mumbai (India) and used without any pretreatment. Epichlorohydrin was employed as a crosslinker for starch and used as received. Silicon oil (Research Lab, Mumbai, India) was used as an oil phase. Other chemicals like $FeCl_2{\cdot}H_2O$, $FeCl_3{\cdot}6H_2O$ (Merck, Mumbai India), and solvents used were of standard quality (A R) grade. Cisplatin was used as a model anticancer drug and obtained from Dabur Pharma Ltd. New Delhi, India.

2.2. Methods (preparation of magnetic starch nanoparticles)

The iron oxide impregnated starch nanoparticles were prepared by emulsion crosslinking method. In general, magnetic nanoparticles production involves co-precipitation of ferrous and ferric salts in an alkaline medium with continuous stirring as shown below:

$$2FeCl_3 + FeCl_2 + 8NH_4OH \rightarrow Fe_3O_4 + 8NH_4Cl + 4H_2O \quad (3)$$

In the present study, the 'aqueous phase' of starch was prepared by dissolving a definite amount of starch in boiling distilled water, to obtain a clear solution. To the above solution, 11.1 mM of $FeCl_2{\cdot}H_2O$, $FeCl_3{\cdot}6H_2O$ salts and 60 mL of silicon oil were added, and the resulting solution was mixed with vigorous shaking for 1 h to from a stable suspension. To this suspension was added a dropwise suspensions of NH_4OH and epichlorohydrin prepared in silicon oil with constant shaking on a rotatory shaker at 3000 rpm. The crosslinking reaction was allowed to proceed for 5 h and the crosslinked iron oxide impregnated starch nanoparticles were prepared. The prepared nanoparticles were allowed to stand for 24 h to get stabilized and then washed with toluene and acetone. Thoroughly washed nanoparticles were dried and stored in polyethylene bags.

3. Characterization

3.1. Physicochemical characterization

3.1.1. FTIR spectral analysis

FTIR spectral analysis was carried out for structural characterization of nanoparticles. The FTIR spectra of crosslinked nanoparticles were recorded on a FTIR spectrophotometer in the range of 4000–400 cm^{-1} (8400S, Shimadzu spectrophotometer).

3.1.2. X-ray diffraction analysis

The X-ray diffraction studies of the nanoparticles were carried out on Philips PW1820 powder diffractometer. The diffraction data were collected from 10° to 60°, 2θ values with a step size of 0.02 and counting time of 2 s $step^{-1}$. The average crystallite size of iron oxide impregnated nanoparticles of starch was estimated using Debye-Scherer's formula.

3.1.3. TEM analysis

Transmission electron microscopy (TEM) was performed by using a Morgagni-268-D transmission electron microscope with an acceleration voltage of 80 kV. The samples for the TEM measurements were prepared by dispersing a drop of the sample suspension on Formvar-coated C grids.

3.1.4. Vibrating sample magnetometry (VSM) analysis

A vibrating-sample magnetometer (VSM) was used to study the magnetic properties of iron oxide impregnated starch nanoparticles at room temperature. The coercivity (H_c), the remnant magnetizations (M_r) and the saturation magnetizations (M_s) of prepared nanoparticles were determined from the hysteresis loops produced by the VSM.

3.1.5. Surface potential (zeta potential) measurements

The zeta potential of nanoparticles is commonly used to characterize the surface charge properties of nanoparticles (Chouhan & Bajpai, 2009a,b). In order to understand the nature of the drug and magnetic nanoparticles interaction, zeta potential studies were performed with a digital potentiometer (Model No. 118, El product, Mumbai, India).

3.2. Biopharmaceutical characterization

3.2.1. Swelling studies in nanoparticles

Swelling of nanoparticles was studied by a conventional gravimetric procedure. In a typical experiment, 0.2 g of nanoparticles were allowed to swell in a definite volume (10 mL) of phosphate buffer saline (PBS) taken in a preweighed sintered glass crucible (pore size 5–10 μm) and weighed after a definite time periods by removing excess of phosphate buffer saline by vacuum filtration. The swelling of nanoparticles was monitored continuously up to 15 min after which no weight gain of swollen nanoparticles was recorded (equilibrium swelling conditions). The amount of water imbibed by the nanoparticles was calculated by the following equation (Davidson & Peppas, 1986).

$$\text{Swelling ratio (Sr)} = \frac{\text{Weight of swollen particles (Ws)}}{\text{Weight of dry particles (Wd)}} \quad (4)$$

3.2.2. Loading of drug onto nanoparticles

The incorporation of drugs onto nanoparticles can be performed by one of the following ways: (i) either by adding the drug into the feed mixture during the preparation of the device, (ii) or by allowing the device to swell in the drug solution until equilibrium swelling is reached (Chouhan & Bajpai, 2009a). In the present work, however, the later method was adopted as in the former method purification of the loaded device always remains a problem.

A varying degree of cisplatin loaded nanoparticles were prepared by allowing 0.1 g of nanoparticles to swell until equilibrium in freshly prepared drug solutions (10 mL). The percent loading of nanoparticles was calculated by the following equation:

$$\%\ \text{Loading} = \frac{W_d - W_o}{W_o} \times 100 \quad (5)$$

where W_d and W_o are the weights of loaded and unloaded nanoparticles, respectively.

3.2.3. In vitro release experiments

In vitro release study of the cisplatin-loaded nanoparticles was carried out by placing loaded nanoparticles (0.2 g) in a test tube containing a definite volume (10 mL) of phosphate buffer saline (PBS) as the release medium (pH 7.4) (1.2 mM KH_2PO_4, 1.15 mM Na_2HPO_4, 2.7 mM KCl, 1.38 mM NaCl). The resulting suspension was gently shaken for a definite time period (1.5 h) and 5 mL supernatant was withdrawn at predetermined time intervals (30 min) from the suspension medium replacing it with the same volume of fresh PBS. The amount of cisplatin released from the polymeric magnetic nanoparticles was measured spectrophotometrically at 240 nm (Shimandzu 1700 Pharma Spec.) and the released amount of drug was determined from the calibration plot.

3.2.4. Release kinetics

The release of drug from polymeric nanoparticulate systems is usually considered as a combination of Fickian (diffusion) and non-Fickian movements of drug molecules through polymer chains. Release from nanoparticulate system is predominantly diffusion controlled. In the present study the kinetic data were analyzed with the help of the following equation (Chairam & Somsook, 2008), which could be helpful in determining the possible mechanisms of the release process,

$$\frac{W_t}{W_\infty} = Kt^n \quad (6)$$

where W_t and W_∞ are the amounts of the drug released at time t and at infinity time (equilibrium amount of drug released), respectively, and K is rate constant. For evaluating the diffusion constant of loaded drugs, the following equation can be used:

$$\frac{W_t}{W_\infty} = \left(\frac{Dt}{\pi L^2}\right)^{0.5} \quad (7)$$

where D is the diffusion constant of the drug and L being the diameter of the dry nanoparticles.

3.2.5. Magnetically induced in vitro release experiments

Magnetically induced in vitro release of the encapsulated drug were carried out by placing the dried and loaded nanoparticles in a test tube containing a definite volume of PBS (pH 7.4) as the release medium under gentle shaking for a definite time period and in the absence and presence of magnetic field (MF) (Electromagnet Model EM-07). The average MF applied to the nanoparticles was 300 G, which was measured by using a Digital Gauss meter (Model DGM-20). At pre determined time intervals (15 min) 5 mL supernatant was withdrawn from the release medium and replaced with fresh PBS. The amount of drug released from particles was measured spectrophotometrically at 240 nm (Shimandzu 1700 Pharma spectrometer) with the help of a calibration plot.

3.2.6. Chemical stability of drug

In order to check the chemical stability of entrapped drug in different release media, the UV spectral study (Shimandzu 1700 Pharma Spec) was performed which involves recording the UV spectra of pure cisplatin solution and released fractions at different pH and different time periods, respectively.

3.2.7. Statistical analysis

All experiments were done at least thrice and the data and figures have been expressed along with respective standard deviations and error bars, respectively.

4. Results and discussion

4.1. Characterization of nanoparticles

The FTIR spectroscopy of native starch nanoparticles (a), iron oxide impregnated nanoparticles (b), drug loaded nanoparticles (c) and pure drug cisplatin (d) was carried out to confirm the presence of characteristic functional groups of components as shown in Fig. 2(A) (a–d, respectively). The IR spectra shown in Fig. 2(A) (a) clearly mark the evidence for the presence of starch observed by the peaks at 3581 cm^{-1} due to the O–H stretching vibration. Additional multiple bands appear at a lower frequency in the range 3000–3500 cm^{-1} at the expense of the starch hydroxyl groups, C–H stretching at 2920 cm^{-1}, O–H bending at 1259 cm^{-1}, C–O stretching

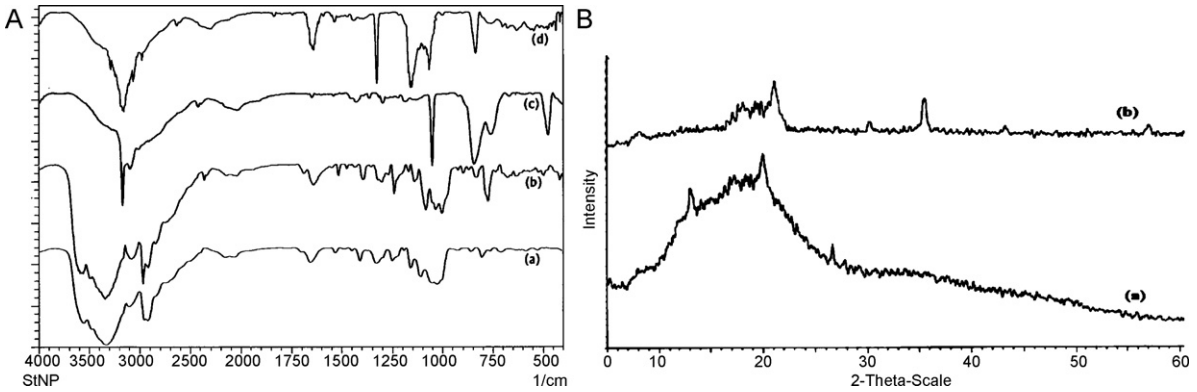

Fig. 2. (A) FTIR spectra of – (a) starch nanoparticles (b) iron oxide impregnated starch nanoparticles (c) cisplatin loaded iron oxide impregnated starch nanoparticles and (d) pure cisplatin drug and (B) X-ray diffraction pattern of – (a) starch nanoparticles and (b) iron oxide impregnated starch nanoparticles.

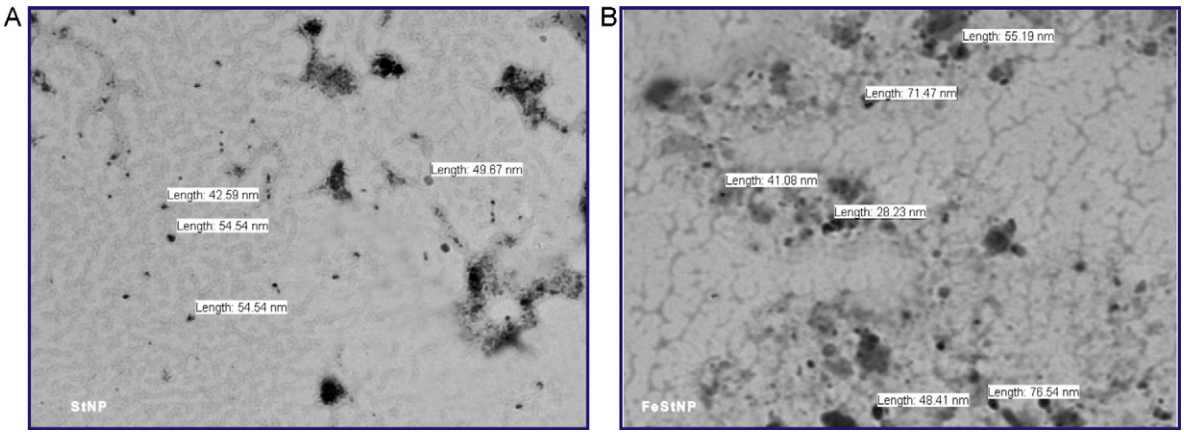

Fig. 3. (A) TEM image of crosslinked starch nanoparticles and (B) the TEM image of iron oxide impregnated starch nanoparticles.

at 1026 cm^{-1} and a prominent C–O–C stretching of the glycosides bonds at 1105 cm^{-1} (typical for starch). The spectra 2A (b) show the presence of iron oxides as evident from the peaks observed at 526–418 cm^{-1}. The spectra 2A (c) show the presence of cisplatin-loaded nanoparticles as evident from the two sharp peaks observed at 677 cm^{-1} and 538 cm^{-1} (due to torsional oscillation of $-NH_3^+$ group) and the spectra 2A (d) show the pure drug of cisplatin as evident from the peaks observed at 2370 cm^{-1},1539 cm^{-1}, 1134 cm^{-1}, 1024 cm^{-1} due to $-CH_2$ wagging, 934 cm^{-1} due to –NH wagging, and 499 cm^{-1} due to Pt–N stretching vibrations, respectively.

The XRD analysis is an essential tool for determination of crystallinity of the material (Gupta & Bajpai, 2010). The well defined X-ray diffraction patterns indicate the formation of highly crystalline iron oxide nanoparticles. The XRD pattern of the prepared native starch nanoparticles and iron oxide impregnated starch nanoparticles is shown in Fig. 2(B) (a and b), respectively. The spectral pattern for native iron oxide nanoparticles is shown in Fig. 2(B) (b) which indicates the characteristics peaks of iron oxide impregnated starch nanoparticles at 21.4° and 37.1°. The X-ray diffraction patterns of the starch nanoparticles shown in Fig. 2(B) (a) indicate the characteristic peak for starch at 20.2°, which clearly reveal that iron-oxide is impregnated into starch nanoparticles. The mean grain size of the iron oxide impregnated starch nanoparticles was calculated using Debye-Scherrer formula (Gupta & Bajpai, 2010) as given in Eq. (8)

$$d = \frac{k\lambda}{\beta \cos \theta} \tag{8}$$

where d is the mean grain size, k is the shape factor (0.9), β is broadening of the diffraction angle and λ is diffraction wavelength (1.54 Å). The estimated average grain size of iron oxide impregnated starch nanoparticles was found to be 6.8 nm.

The amorphous and crystalline natures of the iron oxide impregnated starch nanoparticles were determined in terms of degree of crystallinity. The numerical formula to calculate the percent crystallinity of nanoparticles is given in the following equation:

$$X_c = \frac{A_c}{A_a + A_c} \times 100 \tag{9}$$

where A_c and A_a are the area of crystalline and amorphous phases, respectively. The crystallinity of the material has been calculated using the formula given in Eq. (9). The % crystallinity of native starch was found to be 43.8%, while for iron oxide impregnated starch nanoparticles it is about 67.5%. The observed results are quite obvious as being a semi crystalline biopolymer, starch shows lesser crystalline nature then the material containing iron-oxide within the starch matrix.

In order to investigate the size and morphology of prepared nanoparticles, transmission electron micrograph (TEM) images were recorded as shown in Fig. 3(A and B), respectively which represent the size of nanoparticles. It is clear from the images (A) and (B) that the size of starch and iron oxide-impregnated nanoparticles varies from 28 nm to 118 nm and 26–148 nm, respectively. The images also indicate that the shape and size of nanoparticles are not uniform.

4.2. Magnetization studies

In order to explore the nature of magnetic behavior of the prepared nanoparticles, variation in magnetic moments of prepared iron oxide nanoparticles was investigated as a function of varying magnetic fields. The results are shown in Fig. 4 which shows a typical magnetization (M) *versus* the applied magnetic field (H) plot at room temperature (27 °C). Fig. 4 is the magnetization curve of magnetite nanoparticles, showing superparamagnetic property (i.e., no remanence effect) and saturation magnetization of about 58 emu/g of magnetite nanoparticles. The obtained values are lower than the reported values of 92–100 emu/g for magnetite (Fe_3O_4) nanoparticles (Morales, Jain, & Labhasetwar, 2005) and may exist attributed to the fact that, below a critical size, nanocrystalline magnetic particles may exist as single domain and show the unique phenomenon of superparamagnetism (Chin, Zakaria, Ahamd, Abdullah, & Jani, 2006).

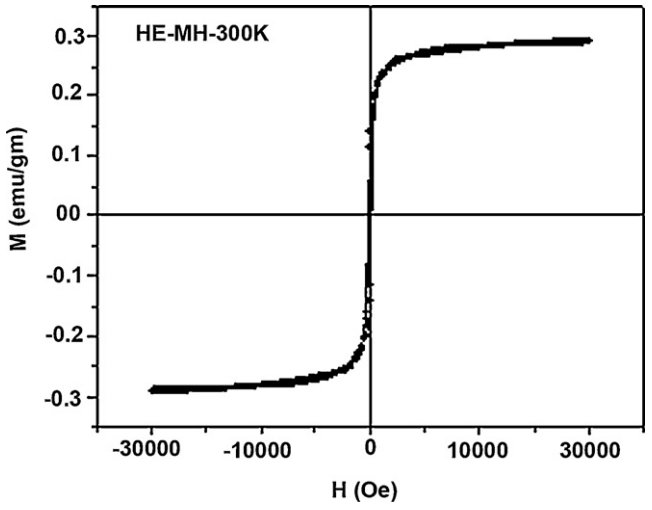

Fig. 4. Hysteresis curve of iron oxide impregnated starch nanoparticles obtained by VSM measurements.

Table 1
Effect of varying compositions of nanoparticles on their swelling.

Sample no.	Starch (g)	Epichlorohydrin (mM)	Iron chloride (mM)	Swelling ratio	
				No magnetic field	Magnetic field
1	3.0	102.28	11.1	2.6 ± 0.082	3.2 ± 0.068
2	4.0	102.28	11.1	2.8 ± 0.094	3.33 ± 0.040
3	5.0	102.28	11.1	3.6 ± 0.088	4.65 ± 0.098
4	6.0	102.28	11.1	2.75 ± 0.078	3.8 ± 0.086

4.3. Effect of swelling on nanoparticles

The effect of increasing starch content on the swelling characteristics of the iron oxide impregnated starch nanoparticles has been investigated by varying the amount in the range 3.0–6.0 g in the feed mixture in the presence and absence of magnetic field. The results are summarized in Table 1, which clearly indicate that the swelling of starch initially increases in the range of 3.0–5.0 g and thereafter decrease in swelling is noticed. The results may be attributed to the fact that starch is a hydrophilic biopolymer, and its increasing amount in the particles will obviously increase the hydrophilicity of the nanoparticles and thus an increase in the swelling ratio is expected (Bajpai & Bhanu, 2007). However, beyond 5.0 g of starch content, the observed decrease in swelling ratio may be due to the enhanced compactness of the particles and greater interaction between macromolecule chains of starch nanoparticles.

4.4. Effect of % loading on cisplatin release

In the present study physical loading was followed which involved swelling of preweighed nanoparticles into the drug solution of concentration ranging from 10% to 80%. The release profile of nanoparticles loaded to different extent are shown in Fig. 5(A), which clearly indicate that initially up to 20% drug loading cumulative release increases, while beyond this there is a fall in the release rate. The observed increase in drug release is due to the reason that higher loading of drug facilitates a faster movement of the solvent front (PBS) that penetrates the surface of the loaded nanoparticles and, therefore, results in a greater drug release (Kim, Bae, & Okano, 1992). However beyond 20% loading of drug, a fall is noticed in the extent of release, which could be explained by the fact that, at much greater loading of drug, voids of the nanoparticles shrinks due to accumulation of the drug molecules within the particles and this restrains the diffusion of water molecules into the loaded nanoparticles and results in a suppressed release of drug (Bajpai & Mishra, 2005).

4.5. Surface potential measurements

The zeta potential measurements were used to characterize the surface charge properties. The results are shown in Fig. 5(B), which clearly indicates that upon loading of iron oxide onto starch nanoparticles surfaces, a net increase in positive potential was

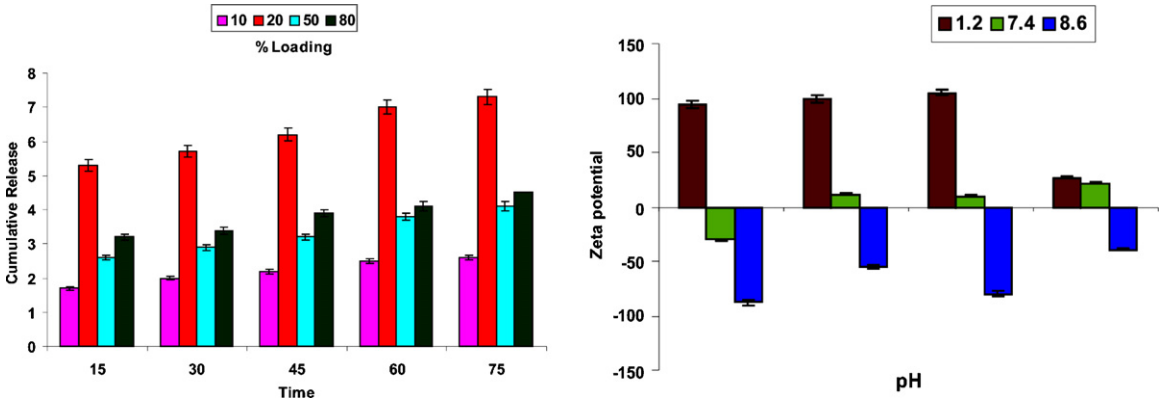

Fig. 5. (A) Zeta potential of cisplatin loaded iron oxide impregnated starch nanoparticles at various pH and (B) effect of % loading of cisplatin on its release profiles from loaded nanoparticles of definite composition [starch] = 5 g, [epichlorohydrin] = 102.28 mM, [ferrous and ferric salt] = 11.1 mM.

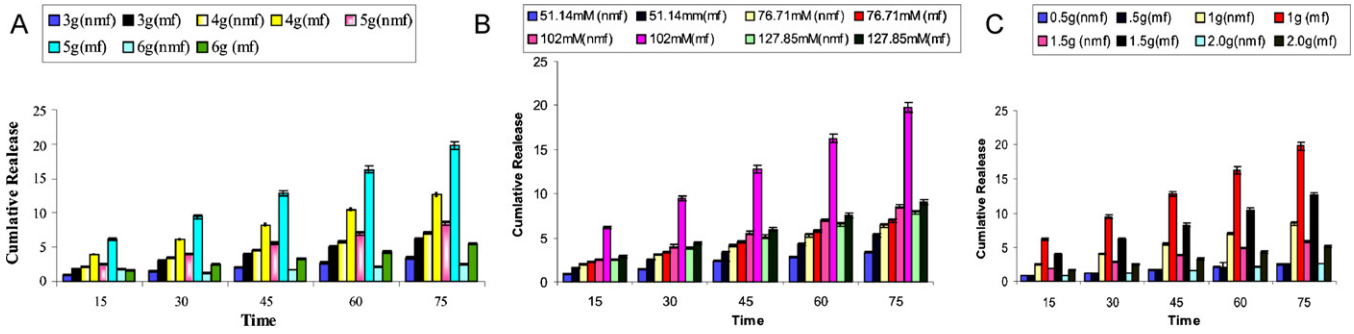

Fig. 6. (A) Effect of starch content of the nanoparticles of the release profile of cisplatin, (B) effect of epichlorohydrin on the release profile of cisplatin and (C) effect of iron oxide of on the release profile of cisplatin of definite amount of starch = 5 g, epichlorohydrin = 102.28 mM, ferrous and ferric salt = 11.1 mM.

noticed. This property may be explained by measuring the zeta potential of iron oxide nanoparticles as shown in Fig. 5(B). The zeta potential value at pH 1.8 is 305 mV, pH 7.4 is 10 mV and pH 8.6 is −55 mV. The decrease in positive potential in alkaline pH shows that iron-oxides were in anionic form FeO^-, while increase in positive potential in acidic pH indicates that iron oxide is present as $FeOH_2^+$ (Laurence et al., 2007). Similar type of results has been reported elsewhere (Guo, LI, Zhang, Jing, & Wang, 2009). Zeta potential of cisplatin loaded nanoparticles with higher loading was more electropositive as reported elsewhere also (Yan & Gemeinhart, 2005).

4.6. Effect of starch on release of cisplatin

In the present study the size and morphology of nanoparticles are greatly determined by factors such as concentration of starch and epichlorohydrin in the feed mixture (Bajpai & Bhanu, 2007). The effect of starch on the drug release has been investigated by varying the amount of starch in the range of 3.0–6.0 g in the feed mixture. The release study was carried out in both conditions (with and without magnetic field). The release and swelling results are displayed in Fig. 6(A), which clearly indicate that the cumulative release of cisplatin increases with increasing starch content in the range of 3.0–5.0 g and thereafter a decrease in release was noticed. The results may be attributed to the fact that starch is a hydrophilic biopolymer, and its increasing amount in the particles will obviously increase the hydrophilicity of the nanoparticles and thus an increase in drug release is expected. However, beyond 5.0 g of starch content, the observed decrease in drug release may be due to an enhanced compactness of the particles and greater interaction between macromolecular chains of starch nanoparticles.

4.7. Effect of cross-linker (epichlorohydrin) on release of cisplatin

In the present study epichlorohydrin has been used to crosslink starch in the concentration range of 24.4–127.85 mM in the feed mixture. The results are depicted in Fig. 6(B) which shows an increase in drug release with increase in concentration of crosslinker in the range 24.4–102.28 mM. The observed increase in released drug is due to the fact that epichlorohydrin is a low molecular weight crosslinking agent of starch, which at its two terminals crosslink with the hydroxyl groups of starch. Thus, a crosslinked starch network could be imagined as ultrahigh molecular weight starch molecules that contains wide pore sizes in its structure and, therefore, possesses an abnormal capacity of accommodating into the network. Thus, capacity to imbibe increasing number of drug molecules results in an increased release which is clearly shown in Fig. 6(B). The obtained increase in release permits a greater number of molecules to diffuse out of material and pass into the release medium.

However, beyond 102.28 mM of epichlorohydrin, the network of starch is highly crosslinked, which consequently reduces the free volume accessible to the penetrant drug molecules. Similar types of results have also been reported by other workers (Bajpai & Shrivastava, 2005).

4.8. Effect of iron-oxide on cisplatin

To investigate the effect of iron-oxide on release of the drug, the concentration of iron chloride was varied in the feed mixture over the range 5.5–22.2 mM. The results are depicted in Fig. 6(C), which reveals an increase in drug release with increase in concentration of iron chloride in the range of 5.5–11.0 mM. The observed increase in released drug is due to the fact that Fe^{2+}/Fe^{3+} ions interact with the crosslinked starch nanoparticles and such type of binding of ions to the crosslinked starch nanoparticles results in an enhanced drug

Table 2
Data showing the amount of released cisplatin at various pH and temperature and in different biological fluids.

S. no.	Time in min	Cumulative release (mg/mL)													
		pH						Temperature			Biological fluid				
		1.8 (nmf)	1.8 (mf)	7.4 (nmf)	7.4 (mf)	8.6 (nmf)	8.6 (mf)	15 °C (mf)	25 °C (mf)	42 °C (mf)	NaCl (mf)	Urea (mf)	KI (mf)	Glucose (mf)	PBS (mf)
1.	15	2.5	2.9	2.1	2.5	1.3	1.6	1.1	1.4	1.6	0.6	0.5	0.8	1.1	2.5
2.	30	4.05	4.8	3.1	3.6	2.6	2.8	1.75	2.2	2.45	0.92	0.75	1.2	1.55	4.05
3.	45	5.55	5.9	4.2	4.8	3.4	3.9	2.65	3.05	3.53	1.23	1.05	1.65	2.18	5.55
4.	60	7.0	7.8	5.2	5.9	4.0	4.6	3.0	3.9	4.69	1.57	1.3	2.05	2.78	7.0
5.	75	8.55	9.4	7.1	7.3	5.2	5.4	3.95	4.99	5.74	1.94	1.59	2.53	3.48	8.55

Table 3
Data showing the release exponents and diffusion coefficients obtained under varying experimental conditions.

Sample no.	Starch (g)	Epichlorohydrin (mM)	Iron chloride (mM)	pH	Diffusion coefficient $D \times 10^{-2}$ (cm^2/s)	n	R^2	Mechanism
1	3.0	102.28	11.1	7.4	1.25	0.63	(0.998)	Anomalous
2	4.0	102.28	11.1	7.4	1.85	0.63	(0.996)	Anomalous
3	5.0	102.28	11.1	7.4	1.85	0.42	(0.997)	Fickian
4	6.0	102.28	11.1	7.4	1.44	0.63	(0.995)	Anomalous
5	5.0	24.4	11.1	7.4	1.64	0.66	(0.998)	Anomalous
6	5.0	51.14	11.1	7.4	2.3	0.53	(0.999)	Anomalous
7	5.0	76.71	11.1	7.4	1.64	0.63	(0.999)	Anomalous
8	5.0	127.85	11.1	7.4	1.85	0.63	(0.999)	Anomalous
9	5.0	102.28	5.5	7.4	1.85	0.44	(0.998)	Fickian
10	5.0	102.28	16.6	7.4	1.85	0.60	(0.997)	Anomalous
11	5.0	102.28	22.2	7.4	1.64	0.66	(0.999)	Anomalous
12	5.0	102.28	11.1	1.8	1.44	0.41	(0.987)	Fickian
13	5.0	102.28	11.1	8.6	1.64	0.58	(0.998)	Anomalous

release. Beyond that on further increase in the amount of iron chloride drug release decreases. The observed decrease in release rate may be attributed to the fact that with increasing percent loading the pore size of nanoparticles becomes smaller due to accumulation of drug molecule within the particles and this restrains the diffusion of water molecules into the loaded nanoparticles (Kou & Liang, 2011).

4.9. Effect of MF variation on drug release

The influence of magnetic field on drug release is measured by varying MF in the range of 100–300 G. The obtained results show that with increasing strength of magnetic field the drug release increases, and the maximum drug release was observed at 300 G. The observed results may be attributed to the fact that magnetic moment of material M is proportional to the applied field H (Eq. (2)).

The possible reason for the observed increase in drug release upon application of the magnetic field may be that under the applied field the magnetic nanoparticles of drug carrier get aligned with the applied field.

When loaded nanoparticles are exposed to a high magnetic field, the monodomain nanoparticles generate heat through oscillation of magnetic moments and subsequently enlarges the nanostructure of the polymeric matrix to produce porous channels that cause enhanced diffusion process and, as a consequence, the drug releases easily. Similar type of results has also been reported elsewhere (Gupta & Bajpai, 2010).

4.10. Effect of biological fluids

The influence of solutes on the release kinetics of cisplatin was examined by performing release experiments in the presence of solutes such as urea, sodium chloride (NaCl), potassium iodide (KI), D-glucose and PBS in physiological fluids. The results are shown in Table 2 which indicates that in comparison to PBS the amount of released cisplatin decreases in other simulated biological fluids. The possible reason for the observed lower release of drug in these solutes is due to the presence of salt ions in the release medium which lowers the osmotic pressure in the system thus resulting in lower extent of release.

4.11. Effect of pH on cisplatin

In the present investigation, the release dynamic of the drug cisplatin has been observed under varying pH conditions as found in the GIT [e.g., stomach (gastric juice) 1.0, and small intestine 7.5–8.6]. The wide range of pH allows a specific drug to be delivered to a targeted site only. The drug-release kinetic for cisplatin loaded iron oxide impregnated starch nanoparticles was studied at three different pH conditions (1.8, 7.4 and 8.6). The results summarized in Table 2 indicate that the drug release was faster as acidic pH value than at basic pH as a consequence of weaken binding between drug and the partially nutrilised carboxyl group in iron oxide impregnated starch nanoparticles (Choubey & Bajpai, 2010). However, in the 7.4 and 8.6 pH nearly similar drug release was observed which can be explained by the fact that the cisplatin drug (amphoteric in nature) and COOH groups undergo a partial hydrolysis to produce COO^- anionic groups these ions causes repulsive forces to operate among themselves and thus, macromolecules chains undergo a fast relaxation which facilitates the penetration of water into the loaded nanoparticles and subsequently enhances the amount of drug released (Flory, 1953).

4.12. Effect of temperature on cisplatin release

Temperature has a direct influence on the release behavior of nanoparticles as it affects the segmental mobility of the hydrogel chains, diffusion of penetrant water molecules and expulsion of drug molecules. In the present study, the effect of temperature on the drug release through starch nanoparticles has been investigated by varying the temperature of the release medium in the range of 15–42 °C. The results summarized in Table 2 clearly show that with increasing temperature, the drug release increases.

The observed increase in the released amount of drug can be explained by the fact that with increasing temperature, the network chains also undergo faster relaxation due to an increased kinetic energy and thus facilitate the water sorption process (Chouhan & Bajpai, 2009a,b). The observed increase in drug release may be attributed to the fact that with increasing temperature the H-bonds between the drug molecules and network chains are broken, thus converting bound water into free water. This results in a higher loading of nanoparticles and, consequently, an increase in the released amount of cisplatin is observed.

4.13. Chemical stability of drug

The chemical stability of the entrapped drug was investigated by recording the UV spectra of pure drug and released drug in release media, i.e., at pH 7.4. A comparison of the two curves (not shown) clearly reveals that the spectra are almost identical thus suggesting that no significant changes in chemical and bioactivity of the drug occurred following the loading and release of drug cisplatin.

4.14. Kinetic analysis of release data: modeling of release mechanism

The drug (cisplatin) loaded iron oxide impregnated starch nanoparticles may be visualized as a three dimensional network of starch macromolecules containing drug molecules which occupy the space available between the network chains. When such drug loaded nanoparticles are allowed to swell in a release medium the solvent (normally water) molecules enter into the nanoparticles network as a result of their diffusion into the nanoparticles matrix and subsequent relaxation of polymer chains take place. The drug molecules dissolve into water and release out through water permeation channels present in the macromolecular network. The diffusion of drug molecules and relaxation of nanoparticle chains determine the type of release mechanism being followed by the drug molecules. It has been laid down by Higuchi equation (Higuchi, 1961) that if $n = 0.43$, the release is diffusion controlled (Fickian), when $n = 0.84$ the release is non-Fickian (or case II), and for n when is in between 0.43 and 0.84, the mechanism becomes anomalous. In some cases n has been found to exceed 0.84 and the mechanism is known as super case II (Siepmann & Peppas, 2001). The value of diffusion coefficient (D) and release exponents (n) have been calculated as described above and are summarized in Table 3. Along with the values of D and n is the respective values of regression coefficients (R^2) have also been expressed. It is clear from the data that the values of R^2 are always greater than 0.99 and, therefore, suggest for a good applicability of release data to Eqs. (6) and (7), respectively.

5. Conclusions

Iron oxide impregnated starch nanoparticles were prepared by emulsion crosslinking method, which effectively delivers antitumor drug cisplatin in the presence and absence of magnetic field via diffusion controlled pathway.

The structural characterization of prepared nanoparticles by FTIR spectral analysis of confirms the presence of functional groups of starch, iron oxide impregnated starch nanoparticles, cisplatin loaded nanoparticles and pure drug. The TEM measurements of the nanoparticles suggest the average particle size 20–80 nm. The % crystallinity of native starch nanoparticles and iron oxide impregnated starch nanoparticles was carried out by XRD measurement, and % crystallinity of native starch was found to be 43.8% and iron oxide impregnated starch nanoparticles is 67.5%. The magnetization studies indicate that the nanoparticles show superparamagnetism which was found to be 58 emu/g for nanoparticles.

It is found that release profiles of drug are greatly influenced by % loading of drug concentration of starch and epichlorohydrin in the nanoparticles. In the case of starch the release of drug initially increase than decrease when the amount of starch is increased from 2.0 to 6.0 g whereas the extent of release decreases beyond 5.0 g of starch content. The release amount of drug increases with increasing crosslinker up to 102.28 mM whereas the extent of release decreases beyond 102.28 mM of crosslinker content.

The release profiles are greatly influenced by pH and temperature of the release medium as well as external magnetic field. The maximum release is obtained at 42 °C in the presence of applied magnetic field. The chemical stability of drug suggests that even in remaining in highly acidic media, the chemical nature of drug does not change. The zeta potential of the drug loaded particles increases at pH 1.8 where as a decreased in zeta potential observed at pH 7.4 and 8.6.

References

Babincova, M., Leszczynska, D., Sourivong, P., Cicmanec, P., & Babinec, P. (2001). Lysis of photosensitized crythrocytes in an alternating magnetic field. *Journal of Magnetism and Magnetic Materials*, *225*, 109.

Bajpai, A. K., & Bhanu, S. (2007). Dynamic of controlled release of heparin from swellable crosslinked starch microspheres. *Journal of Materials Science: Materials in Medicine*, *18*, 1613.

Bajpai, A. K., & Mishra, A. (2005). Preparation and characterization of tetracycline-loaded interpenetrating polymer networks of carboxymethyl cellulose and poly (acrylic acid): water sorption and drug release study. *Polymer International*, *54*, 1347–1356.

Bajpai, A. K., & Shrivastava, J. (2005). In vitro enzymatic degradation kinetics of polymeric blends of crosslinked starch and carboxymethyl cellulose. *Polymer International*, *54*, 1524–1530.

Bertholon, I., Hommel, H., Labarre, D., & Vauthier, C. (2006). Properties of polysaccharides grafted on nanoparticles investigated by EPR. *Langmuir*, *22*, 5485–5490.

Choubey, J., & Bajpai, A. K. (2010). Investigation on magnetic controlled delivery of doxorubincin from superparamagnetic nanocarriers of gelatin crosslinked with genipin. *Journal of Material Science: Material in Medicine*, *21*, 1573–1586.

Chouhan, R., & Bajpai, A. K. (2009a). Release real time *in vitro* studies of doxorubicin release from PHEMA nanoparticles. *Journal of Nanobiotechnology*, *7*, 5.

Chouhan, R., & Bajpai, A. K. (2009b). A swellable in vitro release study of 5-Fluro-uracil (5-FU) from poly-(2-hydroxyethyl methacrylate) (PHEMA) nanoparticles. *Journal of Material Science: Material in Medicine*, *20*, 1103–1114.

Chin, C. H., Zakaria, S., Ahamd, S., Abdullah, M., & Jani, S. M. (2006). Evaluation of water sorption behaviour and in vitro blood compatibility of polyvinyl alcohol based magnetic bionanocomposite. *American Journal of Applied Polymer Science*, *3*, 1750–1760.

Chairam, S., & Somsook, E. (2008). Starch vermicelli template for synthesis of magnetic iron oxide nanocluster. *Journal of Magnetism and Magnetic Materials*, *320*, 2039–2043.

Couvreur, P., Barratt, G., Fattal, E., Legrand, P., & Vauthier, C. (2002). Preparation of magnetic polybutyl cyanoacrylate nanospheres encapsulated with aclacinomycin A and its effect on gastric tumor. *Nanocapsule Technology. Critical Review in Therapeutic Drug Carrier System*, *19*, 99–134.

Davidson, G. W. R., & Peppas, N. A. (1986). Solute and penetrant diffusion in swellable polymer V. Relaxation controlled transport in P (HEMA-co-MMA) copolymers. *Journal of Controlled Release*, *3*, 243.

Ethirajan, A., Schoeller, K., Musyanovych, A., Ziener, U., & Landfester, K. (2008). Synthesis and optimization of gelatin nanoparticles using the miniemulsion process. *Biomacromolecules*, *9*, 2383–2389.

Flory, P. (1953). *Journal principles of polymer chemistry*. Ithaca, NY: Cornell University Press.

Guo, S., LI, D., Zhang, L., Jing, L., & Wang. (2009). Synthesis of nanoparticles for biomedical application. *Biomaterials*, *30*, 1881–1890.

Gupta, R., & Bajpai, A. K. (2010). Magnetically guided release of ciprofloxacin from superparamagnetic polymer nanocomposites. *Journal of Biomaterial Science*, *26*, 1–26.

Higuchi, T. (1961). Rate of release of medicaments from ointments bases containing drugs in suspension. *Journal of Pharmaceutical Science*, *56*, 874.

Hu, F. Q., Wei, L., Zhou, Z., Ran, Y. L., Li, Z., & Gao, M. Y. (2006). One pot green synthesis and bioapplication of L-arginine capped superparamagnetic Fe_3O_4 nanoparticles. *Advanced Material*, *18*, 2553–2556.

Jordan, A., Scholz, R., Wust, P., Hling, H. F., & Felix, R. (1999). Thermosensitive core–shell magnetite nanoparticles surface encapsulated with smart stimuli responsive polymer: Synthesis, characterization and LCST of viable-drug targeting delivery system. *Journal of Magnetism and Magnetic Materials*, *201*, 413–511.

Kim, S. W., Bae, Y. H., & Okano, T. (1992). Hydrogels, swelling drug loading and release. *Pharmacy Research*, *9*, 283–290. doi:10.1023/A:1015887213431

Kou, Y. C., & Liang, C. T. (2011). Catanionic solid lipid nanoparticles carrying doxorubicin for inhibiting the growth of U87MG cells. *Colloids and surface B: Biointerfaces*, *85*, 131–137.

Laurence, D. E., Herve, M., Katel, H., Emilie, M., Claude, L., Pierre, D., et al. (2007). Nanovectors for anticancer agents based on superparamagnetic iron oxide nanoparticles International. *Journal of Nanomedicine*, *2*(4), 541–550.

Morales, M. A., Jain, T. K., & Labhasetwar, V. (2005). Magnetic studies of iron oxide nanoparticles coated with oleic acid and pluronic block copolymer. *Journal of Applied Physics*, *97*(10), 905–913.

Morrish, A. H. (2001). *The physical principles of magnetism*. New York: IEEE Press.

Müller-Schulte, D., & Schmitz-Rode, T. (2006). Thermosensitive magnetic polymer particles as contactless controllable drug carriers. *Journal of Magnetism and Magnetic Materials*, *302*, 267–271.

Prato, M., Kostarelos, K., & Bianco, A. (2008). Functionalized carbon nanotubes in drug design and discovery. *Account of Chemical Research*, *41*(1), 60–68.

Sangeetha, S., Harish, G. L., & Samanta, M. K. (2010). Chitosan-based nanospheres as drug delivery system for cytarabine. *International Journal of Pharmaceutical and Biological Sciences*, *3*(2), 61–64.

Siepmann, J., & Peppas, N. A. (2001). Modeling of drug release from delivery systems based on hydroxypropyl methyl cellulose. *Advanced Drug Delivery Reviews*, *48*, 139–157.

Taylor, A., Krupskaya, Y., Kramer, K., Fussel, S., Klingeler, R., Buchner, B., et al. (2010). Cisplatin-loaded carbon-encapsulated iron nanoparticles and their in vitro effects in magnetic fluid hyperthermia. *Wirth Carbon*, *48*, 2327–2334.

Uchino, H., Matsumura, Y., Negishi, T., Koizumi, F., Hayashi, T., Honda, T., et al. (2005). Cisplatin – incorporating polymeric micelles (NC-6004) can reduce nephrotoxicity and neurotoxicity of cisplatin in rats. *British Journal of Cancer*, *93*, 678–687.
Wang, S. (2009). Ordered mesoporous materials for drug delivery. *Microporous and Mesoporous Material*, *117*, 1–9.
Wang, S. H., Shi, X., Van Antwerp, M., Cao, Z., Swanson, S. D., Bi, X., et al. (2006). Application of nanotechnology in cardio vascular and thoracic diseases. *Advanced Functional Material*, *17*, 3043.
Wenk, E., Wandrey, A. J., Merkle, H. P., & Meinel, L. (2008). Silk fibroin spheres as a plateform for controlled drug delivery. *Journal of Controlled Release*, *132*, 26–34.
Yan, X., & Gemeinhart, R. A. (2005). Cisplatin delivery from poly (acrylic acid-co-methyl methacrylate) microparticles. *Journal of Controlled Release*, *106*, 198–208.
Zhang, H., Mardyani, S., Chan, W. C. W., & Kumacheva, E. (2006). Design of biocompatible chitosan microgels for targeted pH-mediated intracellular release of cancer therapeutic. *Biomacromolecules*, *7*, 1568–1572.